



Effect of surfactants on inactivation of *Bacillus subtilis* spores by chlorine

Tianqi Zhang^a, María Inés Villalba^b, Rongjun Gao^a, Sandor Kasas^{b,c}, Urs von Gunten^{a,d,*}

^a School of Architecture, Civil and Environmental Engineering (ENAC), École Polytechnique Fédérale de Lausanne (EPFL), CH-1015 Lausanne, Switzerland

^b Laboratory of Biological Electron Microscopy (LBEM), École Polytechnique Fédérale de Lausanne (EPFL) and Université de Lausanne (UNIL), CH-1015 Lausanne, Switzerland

^c Centre Universitaire Romand de Médecine Légale, UFAM, Université de Lausanne, 1015 Lausanne, Switzerland

^d Eawag, Swiss Federal Institute of Aquatic Science and Technology (Eawag), CH-8600 Dübendorf, Switzerland

ARTICLE INFO

Keywords:

Surfactants
Chlorine disinfection
Bacillus subtilis spores
Inactivation kinetics
Inactivation mechanisms
Synergistic effects

ABSTRACT

Bacterial spores pose significant risks to human health, yet the inactivation of spores is challenging due to their unique structures and chemical compositions. This study investigated the synergistic effect between surfactants and chlorine on the inactivation kinetics of *Bacillus subtilis* spores. Two surfactants, cocamidopropyl betaine (CAPB) and cetyltrimethylammonium chloride (CTMA) were selected to investigate chlorine disinfection in absence and presence of surfactants. The concurrent presence of both chlorine and surfactant resulted in a moderate reduction in the lag-phases for spore inactivation and negligible increase in the second-order inactivation rate constants. In contrast, when the spores were pre-exposed to surfactants, the lag-phases decreased by about 50 % for both CAPB and CTMA, and the second-order inactivation rate constants during post-chlorination remained constant for CAPB but increased by a factor of 2.3 for CTMA, compared to the control group with phosphate buffer. This synergistic effect became more pronounced with longer surfactant pre-exposure times, reaching its maximum at 3–6 h. The observed synergistic effect suggests that surfactants can potentially enhance the permeability of the coat which is the outmost layer of *B. subtilis* spores and a primary barrier for chemical disinfectants. Tracing a group of *B. subtilis* spores sequentially treated with surfactant and chlorine by atomic force microscopy, a significant decrease in compressive stiffness of the spores was observed due to exposure to surfactants, indicating alterations in the coat by surfactants. The trend in reducing compressive stiffness aligned well with the decrease of lag-phases in inactivation kinetics. Furthermore, CTMA was found to inactivate *B. subtilis* spores through mechanisms different from chlorine. Chlorine primarily inactivated *B. subtilis* spores before damaging the inner membrane of the spores which plays a crucial role in protecting the genetic material stored in the core of the spores. In comparison, CTMA damaged 22 % of the inner membrane for an inactivation efficiency of 99 %. A synergistic effect in damaging the inner membrane was observed when applying CTMA and chlorine simultaneously instead of sequentially.

1. Introduction

Bacterial spores are formed as the result of a stress response during starvation of mother cells of bacteria (McKenney et al. 2013). Once formed, bacterial spores can survive for long time periods (more than centuries) (Cano and Borucki 1995, Sneath 1962) and exhibit extraordinary resistance to adverse environments, such as chemicals, heat, and UV radiation (Nicholson et al. 2000, Setlow 2006). When nutrients become available, the spores germinate from dormancy and return to vegetative growth (Setlow 2003). The extreme persistence and capability to germinate make it challenging to effectively control the risk of

bacterial spores, especially those formed from pathogenic bacteria. In food industries, pathogenic spore-forming bacteria account for a major part of bacterial foodborne diseases and non-pathogenic species also pose challenges for food spoilage (Andersson et al. 1995, Wells-Bennik et al. 2016). In healthcare facilities, bacterial spores formed from human pathogens, such as *Clostridium difficile* pose significant risks to healthcare workers and patients by touching inefficiently disinfected surfaces (Leffler and Lamont 2015, Siani et al. 2011). *Bacillus subtilis* spores serve as model organisms for studying bacterial spores across various fields. In water treatment, *B. subtilis* spores are often used as surrogates for *Cryptosporidium parvum* oocysts, despite some differences in inactivation

* Corresponding author.

E-mail address: urs.vongunten@epfl.ch (U. von Gunten).

<https://doi.org/10.1016/j.watres.2024.122944>

Received 16 September 2024; Received in revised form 3 December 2024; Accepted 8 December 2024

Available online 9 December 2024

0043-1354/© 2024 The Authors. Published by Elsevier Ltd. This is an open access article under the CC BY license (<http://creativecommons.org/licenses/by/4.0/>).

kinetics between the two microorganisms (Larson and Marinas 2003, Morrison et al. 2022). Additionally, *B. subtilis* spores are commonly used to assess the performance of UV disinfection systems (Blatchley III et al. 2005, Bucheli and Egli 2010, USEPA 2006).

The structure and chemical composition of bacterial spores account for their unique resistance properties (Setlow 1993, 1995, 2006). The structures of spores contain multiple layers, from the outermost to the innermost including an exosporium, a coat, an outer membrane, a cortex, a germ cell wall, an inner membrane, and a core (Figure S1, Supporting Information, SI) (Setlow 2014). Among them, the coat and the inner membrane are the main barriers against chemicals, especially oxidizing agents (Leggett et al. 2012, Setlow 2014). The coat of spores consists predominantly of proteins and serves as a sieve for large molecules like lysozyme (Driks 1999). The coat was also identified as a critical barrier against oxidizing chemicals such as chlorine, chlorine dioxide (Young and Setlow 2003), ozone (Young and Setlow 2004), and hydrogen peroxide (Riesenman and Nicholson 2000). This was elucidated by comparing the inactivation efficiencies of wild-type spores with chemically decoated spores or spores that carried a mutation in the gene essential for coat morphogenesis. The resistance to oxidizing chemicals could be partially attributed to detoxifying enzymes, such as superoxide dismutase (Henriques et al. 1998). The inner membrane of spores is remarkably impermeable to even small molecules such as methylamine and water (Cortezzo and Setlow 2005, Sunde et al. 2009). The inner membrane plays a major role in protecting essential genetic material stored in the core against chemicals.

Surfactants which are widely applied in households and industries can serve as antimicrobial agents (Falk 2019). Typically, surfactants interact with bacteria by penetrating bacterial cell walls and solubilizing lipid membranes (Glover et al. 1999, Sharma et al. 2022). So far, two types of surfactants, primary alkyl amines and quaternary ammonium compounds, have been reported to be capable of inactivating bacterial spores via different mechanisms. Primary alkyl amines initiate the germination of spores followed by the inactivation of vegetative cells (Mi et al. 2014, Vepachedu and Setlow 2007). Two possible spore germination mechanisms were proposed. (i) The primary alkyl amines could open a channel in the inner membrane to release dipicolinic acid (DPA), a spore-specific chemical stored in the core which serves as a germinating agent similar to nutrients (Rode and Foster 1961, Vepachedu and Setlow 2007). (ii) Primary alkyl amines could disturb the osmoregulatory function of the cortex of spores and lead to rehydration in the core (Mi et al. 2014). Quaternary ammonium compounds, such as cetyltrimethylammonium bromide, can directly inactivate *Bacillus* spores, partially through damaging the inner membrane (Dong et al. 2019). In contrast, anionic and zwitterionic surfactants are not expected to directly inactivate bacterial spores. However, anionic and zwitterionic surfactants could potentially interact with the coat of spores due to their ability to denature proteins in viral capsids and bacterial membranes (Birnie et al. 2000, Kelleppan et al. 2021, Otzen 2011, Piret et al. 2002).

The inactivation kinetics of *B. subtilis* spores by chemical oxidants applied in water treatment decrease in the order ozone (Driedger et al. 2001) > chlorine dioxide (Chauret et al. 2001) \geq chlorine (Cho et al. 2003, Russell 1990) \gg monochloramine (Larson and Marinas 2003). When oxidants are used in sequence, pre-treatment of *B. subtilis* spores with ozone or chlorine dioxide was observed to enhance their inactivation kinetics during post-chlorination (Cho et al. 2006). The inactivation of spores by chemical disinfectants does not necessarily damage the inner membrane and the genetic material of the spores (Young and Setlow 2003, 2004). Nevertheless, *B. subtilis* spores inactivated by ozone and chlorine are not capable of germinating back to vegetative bacteria. In contrast, the spores inactivated by chlorine dioxide and hydrogen peroxide can initiate germination, but without the ability to replicate after germination (Melly et al. 2002, Young and Setlow 2003, 2004).

Due to the different mechanisms of inactivation of microorganisms, there could be additive or synergistic effects between chemical oxidants

and surfactants when applied together or in sequence. A study conducted in a hospital ward demonstrated that combining a quaternary ammonium chloride with hypochlorite resulted in a significant reduction in the concentration of methicillin-resistant *Staphylococcus aureus* on high-touched surfaces near patients. In contrast, hypochlorite alone proved ineffective in controlling the risk of *S. aureus* contamination (Yuen et al. 2015). Synergistic effects were observed when cetyltrimethylammonium chloride was simultaneously present during *Escherichia coli* inactivation by ozone or chloramine (Voumard et al. 2022). Furthermore, pre-exposure of *E. coli* to CTMA resulted in increased susceptibility to ozone but decreased susceptibility to chloramine (Voumard et al. 2022).

Surfactants discharged into sewers from household and industrial usage can account for ~20–30 % of the dissolved organic carbon in raw sewage (Margot et al. 2015, Matthijs et al. 1999). Current municipal wastewater treatment processes typically reduce surfactant levels from tens of mg/L to hundreds of $\mu\text{g/L}$ through biodegradation and sorption to sludge (Clara et al. 2007, Margot et al. 2015). Nevertheless, the presence of surfactants during the treatment processes may enhance disinfection processes such as chlorination of wastewater. However, the synergistic effects could be more pronounced in special technical systems. For example, a handwashing station uses ultrafiltration and chlorine disinfection to treat and recycle handwashing water (Hands4health 2022). In such a system, hand soap that is present in high concentrations could potentially affect chlorine disinfection efficiency.

The aims of this study were to investigate the effects of combinations of surfactants and chlorine on the inactivation of *B. subtilis* spores. Two surfactants (Figure S2), cocamidopropyl betaine (CAPB) and cetyltrimethylammonium chloride (CTMA), with different hydrophobic alkyl chains (12 versus 18 carbons) and different hydrophilic heads (zwitterionic versus cationic), were tested. First, the inactivation kinetics of *B. subtilis* spores during chlorination in the absence and presence of surfactants were investigated by comparing the lag-phases and the second-order inactivation rate constants. The combined effect was also assessed by applying the surfactants and chlorine sequentially with the spores pre-exposed to surfactants for hours before applying chlorine. *B. subtilis* spores were also investigated by atomic force microscopy (AFM) to assess the changes in the mechanical properties of the coat of the spores caused by surfactants during the pre-exposure. Furthermore, the integrity of the inner membrane of the spores was evaluated during chlorine or CTMA treatment by measuring the releases of DPA from the core of *B. subtilis* spores.

2. Materials and methods

2.1. Chemicals and reagents

Sodium hypochlorite (10–15 % solution) and cetyltrimethylammonium chloride (25 % in water) were obtained from Sigma-Aldrich. Cocamidopropyl betaine (30 % in water) was obtained from Combi-Blocks. Information on the other chemicals and reagents is provided in Table S1 (SI). The concentration of sodium hypochlorite solutions was measured photometrically ($\epsilon_{\text{OCl}_2, 292 \text{ nm}} = 350 \text{ M}^{-1}\text{cm}^{-1}$) (Kumar and Margerum 1987) on a weekly basis using a Shimadzu UV-1800 spectrophotometer. The working solutions for sodium hypochlorite, CAPB, and CTMA were prepared in sterile ultra-purified water (Millipore system (18.2 M Ω)). All glassware (i.e., reactors), pipette tips, and related experimental apparatus were sterilized before use.

2.2. Preparation of cultures of *B. subtilis* spores

Freeze-dried *Bacillus subtilis* bacteria (ATCC 6633) were obtained from ATCC and revived in tryptic soy broth at 30 °C. *B. subtilis* spores were prepared according to Driedger et al. (2001). Briefly, a plate containing Columbia agar was streaked with revived *B. subtilis* bacteria and incubated upside down at 30 °C for 24 h. After incubation, 2 isolated

colonies were transferred into a test tube containing 5 mL of tryptic soy broth. The test tube was then vortexed and incubated at 37 °C for 5 h in a shaker at 20 rpm. To induce sporulation, the *B. subtilis* culture in the test tube was poured onto a CaCl₂-Columbia agar plate prepared by adding 20 mL of 1 % calcium chloride into 1 L of a Columbia agar solution. The plate was incubated at 37 °C for 7 days. After incubation, a thin layer of *B. subtilis* spores was harvested from the top of the CaCl₂-Columbia agar. *B. subtilis* spores were suspended in 10 mL of sterile ultra-pure water and washed three times with water. After washing, the spores were resuspended in 0.5 mL of sterile ultra-pure water and kept at 80 °C for 15 min to remove vegetative cells. The spores stock solution was then stored at 5 °C before use. Following the protocol above, the stock solution contained $\sim 5 \times 10^8$ CFU/mL of *B. subtilis* spores.

2.3. Inactivation kinetics of *B. subtilis* spores by chlorine and surfactants

The inactivation of *B. subtilis* spores in this study refers to the spores losing the capability to germinate or to replicate and form colonies on agar plates after germination. Experiments to investigate the inactivation kinetics of *B. subtilis* spores were conducted by spiking surfactants (25–100 μM of CAPB, 5–100 μM of CTMA) and/or chlorine (0.1 mM = 7.1 mg/L as Cl₂) to 20 mM phosphate buffer (PB, pH 7.0) containing $\sim 5 \times 10^5$ CFU/mL of *B. subtilis* spores. To remove the vegetative bacteria formed during storage, the *B. subtilis* spores-containing stock solution was heated again at 80 °C for 15 min before use. The stock solution was diluted 1000 times to minimize its chlorine demand, meanwhile, ensuring a sufficient initial spores' density to study inactivation kinetics. In the experiments, two different samples were withdrawn to test the spores' viability and chlorine residual. In samples for viability tests, chlorine was quenched with excess sodium thiosulfate ([S₂O₃²⁻]:[chlorine] ≥ 5). The samples were then diluted serially up to 10⁴ times with sterile ultra-pure water before plating. Chlorine residuals were measured by colorimetry with *N,N*-diethyl-*p*-phenylenediamine (DPD) (Table S2) (Baird and Bridgewater 2017). All experiments were conducted with at least two technical replicates.

In viability tests, *B. subtilis* spores were enumerated with the plating method using double-layer agar with minor modifications from Driedger et al. (2001). Plate count (PC) agar was used to prepare agar plates. 0.1 or 0.5 mL of samples containing *B. subtilis* spores were added to 4 mL of soft PC agar (80 % of PC agar) kept at 60 °C. Then the suspension containing the spores-agar mixture was vortexed and poured onto a PC agar plate. After the suspension was solidified, another 4 mL of soft PC agar was added on top. The plate was incubated upside-down at 30 °C for 26 h before counting the colony-forming units (CFU).

2.4. Modeling of kinetic data

The inactivation curves of *B. subtilis* spores during chlorination were modeled using a modified empirical model (Geeraerd et al. 2005, Voumard et al. 2022) (eq. 1). The model takes a lag-phase into account and was modified by considering chlorine exposure (chlorine concentration × contact time) instead of chlorine contact time.

$$N_{c,t} = N_0 \times e^{-k \cdot c \cdot t} \left(\frac{e^{k \cdot S_l}}{1 + (e^{k \cdot S_l} - 1) \times e^{-k \cdot c \cdot t}} \right) \quad (1)$$

where, c is the chlorine concentration (mg/L), t is the chlorine contact time (min), k represents the second-order inactivation rate constant of the spores in the log-linear range (L·mg⁻¹·min⁻¹), S_l corresponds to the lag-phase (mg·L⁻¹·min), N_0 represents the initial spore concentration (CFU/mL), and $N_{c,t}$ represents the spore concentration at a particular oxidant exposure of $c \cdot t$ (CFU/mL). Modeling and analysis were performed with the package “nlsMicrobio” in R (version 2023.03.1) (Baty et al. 2022). In the model, $N_{c,t}$ and the corresponding $c \cdot t$ were obtained experimentally, N_0 , k , and S_l were fitting parameters. Chlorine exposures were calculated by integrating the measured chlorine concentrations as

a function of time (Figure S3). The visualization of the kinetic data was performed using the package “ggplot2” in R.

2.5. Imaging of treated and untreated *B. subtilis* spores with atomic force microscopy (AFM)

The changes of morphology and mechanical properties of *B. subtilis* spores treated with surfactants and/or chlorine were investigated with a JPK NanoWizard 3 AFM (Bruker Nano GmbH, Berlin, Germany) equipped with a Zeiss TE-100 inverted microscope (Bruker Nano GmbH, Berlin, Germany). The AFM was operated in the “quantitative imaging” mode. Data were collected using a cantilever DNP-10 (Bruker Nano Inc., CA, USA) with a nominal spring constant of 0.06–0.1 N m⁻¹. Samples were scanned with a scan area of 7.5 × 7.5 μm². The scans were conducted with the following parameters: 128 × 128 pixels, setpoint: 1nN, Z length: 0.75 μm, and pixel time: 25 ms.

In the experiments, 100 μL of an aqueous spores-containing solution ($\sim 5 \times 10^7$ CFU/mL) was loaded onto a Petri dish that had been functionalized with Corning® Cell-Tak™ according to the commercially recommended protocol. The Petri dish was then incubated at room temperature for 30 min to allow the spores being attached to the Cell-Tak™. After incubation, the Petri dish was washed with ultra-pure water to remove unattached spores before refilling it with ultra-pure water. A group (>10) of randomly selected spores was scanned as the controls of initial cell conditions. After the first scan in water, 10 mM PB (pH 7.0) and 50 μM surfactants (CAPB or CTMA) were spiked to the Petri dish, and the same group of spores was repeatedly scanned three times. Afterwards, 0.1 mM chlorine was dosed to the Petri dish and two consecutive scans were performed again on the same group of spores. After adding surfactants or chlorine, the solution in the Petri dish was mixed by pipetting the solution gently. A few spores were detached from the Cell-Tak™ after adding chlorine. Each round of scans took about 1 h.

Two types of images, the height image and Young's modulus image were processed using the JPKSPM data processing software (version 6.1.198). Using the processed height image, geometric dimensions (length, width, and height) and surface roughness of *B. subtilis* spores were analyzed as explained in Figure S4. Young's modulus, also called elastic modulus is the mechanical resistance of a material while elongating or compressing (Vinckier and Semenza 1998). Here, Young's modulus was used to calculate the compressive stiffness of *B. subtilis* spores (Figure S5). In compressive stiffness calculations, both processed images of height and Young's modulus were saved as black-and-white images and processed with a custom-made dedicated software written in Matlab (version R2023b). The processing consisted in thresholding the height image at a given grayscale value, e.g., >30 (~170 nm), to define a mask with pixels above the threshold. This procedure permitted to select the samples of interest to be analyzed. The mask was then superimposed on Young's modulus image to extract positive matches to be used to calculate the spores' compressive stiffness.

2.6. Test of the integrity of the inner membrane of *B. subtilis* spores with chlorine or CTMA

Dipicolinic acid (DPA) released from the core of spores was monitored to assess the integrity of the inner membrane during the inactivation of *B. subtilis* spores during the application of chlorine and/or CTMA. DPA was measured by fluorimetric detection of the chelate of DPA with terbium (Tb(III)) using fluorescence spectroscopy (Fluorometer CaryEclipse MXD 137) in the phosphorescence mode (Hindle and Hall 1999). Samples containing DPA were mixed with 10 μM terbium chloride (TbCl₃) and 1 M acetate buffer at pH 5.6. The mixed samples were scanned at 271 nm (λ_{excitation}) and 544 nm (λ_{emission}) with a gate time of 4.9 ms and a delay time of 0.1 ms. Experiments to detect DPA were conducted in 1 mM PB (pH 7.0) to minimize the interference of phosphate on the formation of the DPA-Tb^(III) complex (Figure S6). The samples were centrifuged at 5000 g for 6 min before DPA measurement.

The measured DPA concentrations were plotted against the number of lysed spore cells to obtain a correlation between the two parameters (Figure S7). The calibration curve was generated by autoclaving stock solutions of *B. subtilis* spores (121 °C, 30 min) with dilution factors of 2×10^2 – 10^5 (Figure S7). In the experiments with chlorine, excess sodium thiosulfate was applied to quench residual chlorine (Moore et al. 2021). Part of the samples underwent a post-heating process at a sub-lethal temperature of 70 °C for 30 min (Figure S8) to maximize the release of DPA from chlorine-treated spores before DPA measurement (Young and Setlow 2003). In CTMA disinfection experiments, post-heating was not applied due to a lack of a quenching reagent for CTMA.

3. Results and discussion

3.1. Inactivation kinetics of *B. subtilis* spores during chlorination in the absence and presence of the surfactants cocamidopropyl betaine (CAPB) or cetyltrimethylammonium chloride (CTMA)

During chlorine disinfection, the inactivation curves of *B. subtilis* spores present a lag-phase with minor inactivation and a log-linear

phase that follows pseudo-first-order kinetics (Figs. 1 and 2). Similar inactivation characteristics during chemical disinfection have been observed in previous studies (Cho et al. 2003, Driedger et al. 2001, Larson and Marinas 2003). To assess the disinfection efficiency for different experimental conditions, both the lag-phases (S_i) and the second-order inactivation rate constants (k) derived from the log-linear phase were compared (Table S3). All inactivation kinetic experiments were conducted with an initial chlorine dose of 0.1 mM. In this study, PB at pH 7.0 was applied in all experiments, and therefore, interferences of PB on the inactivation kinetics of the spores were investigated first. As shown in Figure S9, a higher second-order inactivation rate constant was observed with 20 mM PB ($0.13 \text{ L}\cdot\text{mg}^{-1}\cdot\text{min}^{-1}$) compared to 1 mM PB ($0.09 \text{ L}\cdot\text{mg}^{-1}\cdot\text{min}^{-1}$). In addition, when the spores were pre-exposed to 20 mM PB for different times (0–51 h) before applying chlorine, the lag-phases for the inactivation were moderately reduced from 57 to ~40 $\text{mg}\cdot\text{L}^{-1}\cdot\text{min}$ with a minor increase in the second-order inactivation rate constants (Table S3). Based on these findings it is critical to conduct kinetic experiments with the same buffer strength so that the data is comparable.

The effect of surfactants on the inactivation kinetics of *B. subtilis*

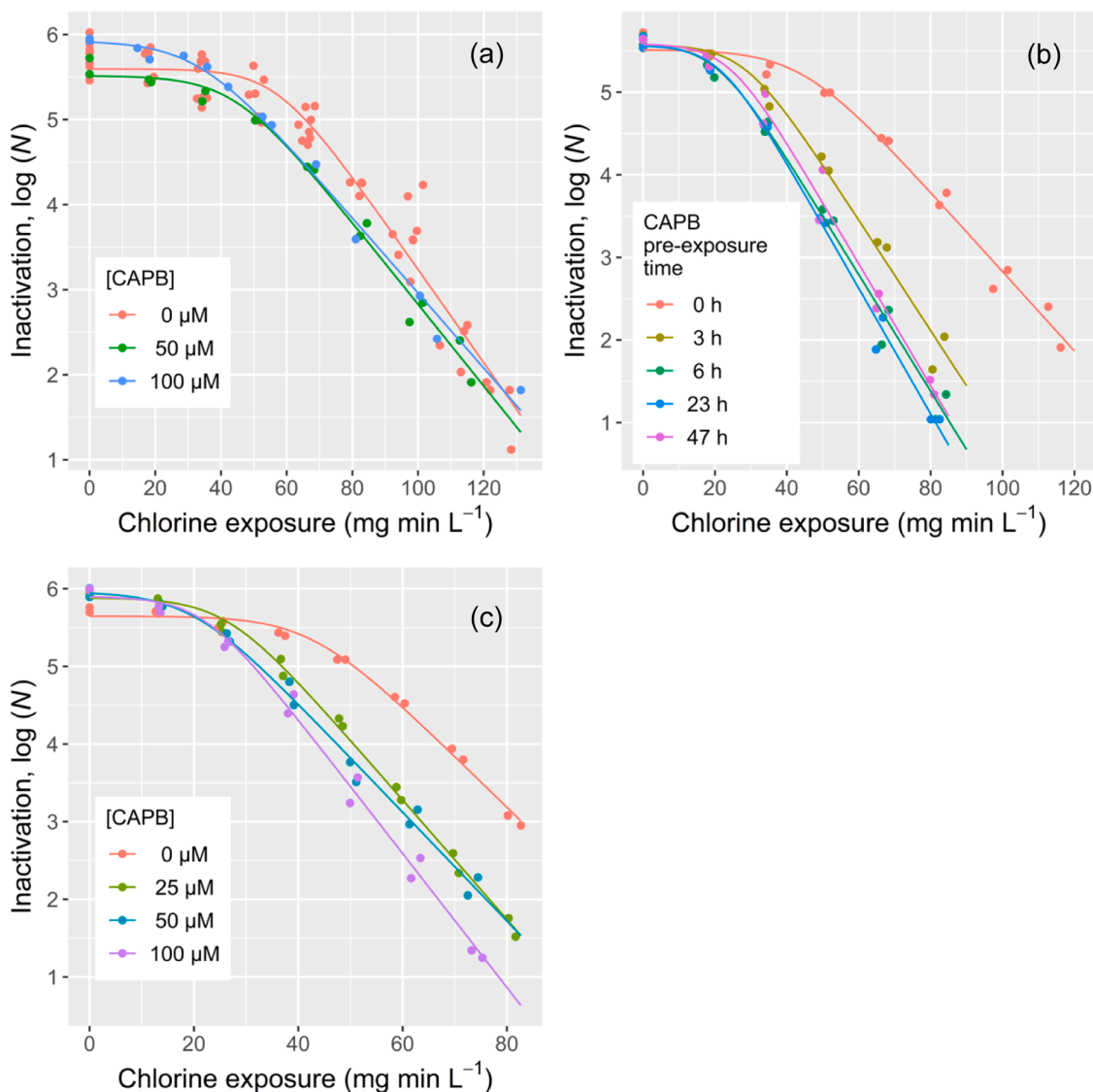


Fig. 1. Logarithmic inactivation of *B. subtilis* spores as a function of the chlorine exposure in absence and presence of CAPB. (a) Simultaneous application of chlorine with varying CAPB concentrations. Sequential application of CAPB and chlorine with (b) varying exposure times to 50 μM CAPB and (c) varying CAPB concentrations for 6 h pre-exposure. Symbols are experimental observations and lines are model fittings using the modified Geeraerd model (eq. 1). Duplicate experiments were grouped when fitting. [*B. subtilis* spores]₀ ≈ 5.8×10^5 CFU/mL (see Table S3 for details), [chlorine]₀ = 7.1 mg/L, 20 mM PB, pH 7.0.

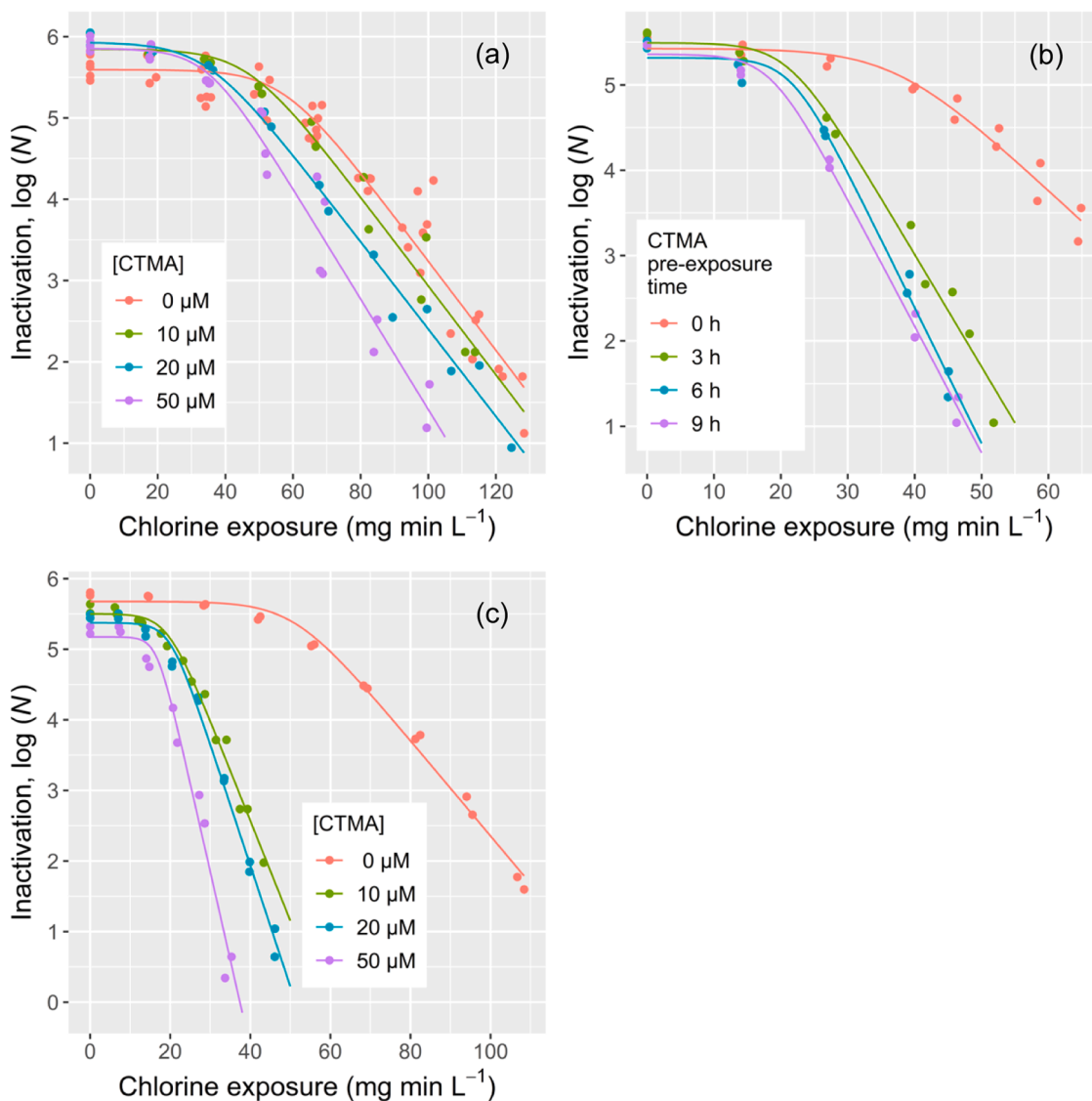


Fig. 2. Logarithmic inactivation of *B. subtilis* spores as a function of the chlorine exposure in absence and presence of CTMA. (a) Simultaneous application of chlorine with varying CTMA concentrations. Sequential application of CTMA and chlorine with (b) varying exposure times to 20 μM CTMA and (c) varying CTMA concentrations for 3 h pre-exposure. Symbols are experimental observations and lines are model fittings using the modified Geeraerd model (eq. 1). Duplicate experiments were grouped when fitting. [*B. subtilis* spores] $_0 \approx 5.6 \times 10^5$ CFU/mL (see Table S3 for details), [chlorine] $_0 = 7.1$ mg/L, 20 mM PB, pH 7.0.

spores by chlorine was tested by simultaneous or sequential addition of surfactant and chlorine. CAPB alone does not inactivate *B. subtilis* spores at concentrations of ≤ 100 μM and exposure times of hours (Figure S10). A concurrent addition of CAPB and chlorine reduced the lag-phases from 57 to 33 $\text{mg}\cdot\text{L}^{-1}\cdot\text{min}$ without a significant change in the second-order rate constants when compared with chlorine alone (Fig. 1a, Table S3). However, when *B. subtilis* spores were pre-exposed to CAPB for hours before applying chlorine, a more pronounced lag-phase reduction (from 44 to ~ 20 $\text{mg}\cdot\text{L}^{-1}\cdot\text{min}$) and a moderate increase in the second-order rate constants (from 0.11 to 0.17 $\text{L}\cdot\text{mg}^{-1}\cdot\text{min}^{-1}$) were observed (Fig. 1b). The synergistic effect of pre-exposure to CAPB on sequential chlorine disinfection reached a maximum for a 6 h pre-exposure time. In the sequential application, an increase of the CAPB concentrations from 25 to 50 or 100 μM did not show an obvious enhancement (Fig. 1c). Notably, the tested concentrations (≤ 100 μM) of CAPB in this study are below the critical micelle concentration of 3.1 mM (El-Dossoki et al. 2020).

Similar tests were performed with CTMA in combination with chlorine (Fig. 2). CTMA alone can inactivate *B. subtilis* spores with 50 μM concentration and exposure times of hours (Figure S11). However, this

inactivation induced by CTMA alone is negligible for exposure times < 20 min which is the maximum exposure time during post-chlorination (refer to post-exposure time in Table S3). A concurrent addition of CTMA and chlorine reduced the lag-phases from 57 to 35 $\text{mg}\cdot\text{L}^{-1}\cdot\text{min}$ without yielding an obvious change in the second-order rate constants (Fig. 2a). For a sequential application, a more pronounced synergistic effect with CTMA and chlorine was observed with the reduction of the lag-phases from 37 to ~ 20 $\text{mg}\cdot\text{L}^{-1}\cdot\text{min}$ and a doubling of the second-order inactivation rate constants from 0.17 to ~ 0.35 $\text{L}\cdot\text{mg}^{-1}\cdot\text{min}^{-1}$ (Fig. 2b). In sequential experiments, the initial spores' populations (N_0) used to calculate log-reduction during post-chlorination were the spores' densities measured after CTMA pre-exposure (refer to N_0 in Table S3). The synergistic effect of pre-exposure to CTMA on sequential chlorine disinfection reached a maximum after a 3 h pre-exposure time. When CTMA and chlorine were applied sequentially, a higher concentration of CTMA led to higher overall inactivation rate constants from 0.16 $\text{L}\cdot\text{mg}^{-1}\cdot\text{min}^{-1}$ in absence of CTMA to 0.33–0.58 $\text{L}\cdot\text{mg}^{-1}\cdot\text{min}^{-1}$ in presence of 10–50 μM CTMA (Fig. 2c, Table S3). Notably, the tested concentrations (≤ 50 μM) of CTMA in this study are below the critical micelle concentration of 0.9 mM (Goronja et al. 2016).

Fig. 3 shows a compilation of the synergistic effects for the sequential application of the surfactants CAPB (red triangles) and CTMA (blue triangles) or PB (black squares) combined with chlorine. The increase of the second-order inactivation rate constants is more pronounced for pre-exposure of the spores to 20 μM CTMA (from 0.17 to 0.35 $\text{L}\cdot\text{mg}^{-1}\cdot\text{min}^{-1}$) than to 50 μM CAPB (from 0.11 to 0.17 $\text{L}\cdot\text{mg}^{-1}\cdot\text{min}^{-1}$) which is similar as PB control (from 0.13 to \sim 0.15 $\text{L}\cdot\text{mg}^{-1}\cdot\text{min}^{-1}$) (Fig. 3a). In contrast, the lag-phases were reduced to a very similar extent when the spores were pre-exposed to either CTMA or CAPB, whereas for PB a smaller effect was observed (Fig. 3b, Table S3). The tested surfactants, CAPB and CTMA, have hydrophobic alkyl chains with different lengths (12 versus 18 C-atoms) and different hydrophilic heads (zwitterionic versus cationic) (Figure S2) which could lead to differences when interacting with microorganisms. For instance, lauryl betaine (similar to CAPB but without an amidopropyl group) and CTMA have minimum inhibitory concentrations of 290 μM and 78 μM , respectively for *E. coli* in broth (Birnie et al. 2000, Voumard et al. 2022).

B. subtilis spores have structures with multiple spore layers (see discussion above and Figure S1) (Setlow 2014). The outmost layer of the coat containing a large fraction of spore proteins and detoxifying enzymes plays an essential role in protecting spores against chemical disinfectants (Henriques et al. 1998, Henriques and Moran 2007, Setlow 2014). The observed lag-phases in the inactivation kinetics curves of *B. subtilis* spores are likely attributed to enzymatic detoxification associated with the coat of the spores. To effectively inactivate spores, particularly hindering the germination process of spores, chlorine is expected to penetrate the coat and damage essential components within. In the sequential application, surfactants applied during pre-exposure may potentially alter the structure of the coat, thus reducing the lag-phase and facilitating the penetration of chlorine. Enhanced kinetics were observed only when surfactants interacted with spores for hours prior to chlorine addition. For simultaneous additions of surfactant and chlorine, there was not enough time to precondition the spores before chlorination, thus enhanced inactivation kinetics were not observed.

3.2. Morphological changes of *B. subtilis* spores after exposure to surfactants

To investigate the changes that surfactants could induce on *B. subtilis*

spores, the spores were scanned by AFM which is widely used to characterize the morphology and mechanical properties of microorganisms, including bacterial spores (Chada et al. 2003, Voumard et al. 2020, Zolock et al. 2006). Here, we traced and scanned the same individual spores of *B. subtilis* during a sequential treatment by surfactants (CAPB and CTMA for \leq 3 h) followed by chlorine (\leq 2 h) (Figures 4 and S12) with a focus on assessing the changes of geometric dimensions, surface roughness and compressive stiffness of the spores. Control experiments were conducted by pre-exposing the spores to PB for 3 h before adding chlorine (Figure S13). Figures 4, S12, and S13 show some labeled and unlabeled spores. Only the labeled spores were used for quantitative assessment. The unlabeled spores were not considered because they completely lost their integrity or were detached from the Cell-Tak™ during the treatments.

In the assessment of dimensional changes during the sequential treatment with surfactant or PB followed by chlorination, changes were observed on some traced spores, however, without a clear trend. During pre-exposure to CAPB (Fig. 4), three individual spores among nine were observed to be reduced by $>20\%$ in size (Table S4). In contrast, spores exposed to CTMA or PB (Figures S12 and S13) had small ($<15\%$) dimensional changes (Table S4). During post-chlorination, spores pre-treated with CAPB or PB tended to reduce sizes, but spores pre-treated with CTMA tended to have a dimensional increase (Table S4). Since these changes were small and not very consistent, they are not further evaluated. A scan of a larger population of the spores would be needed to further understand these dimensional changes. No changes in the surface roughness of the spores were observed for any tested conditions (data not shown).

The compressive stiffness of *B. subtilis* spores was assessed by monitoring the variations of Young's modulus during the surfactant-chlorination or PB-chlorination treatments as shown in Figures 4, S12, and S13. Calculated values of Young's modulus are presented in Table S4, Figures 5 and S14–16 in which yellow represents control in water, green represents pre-exposure to surfactant and/or PB, and red represents post-chlorination. In the control experiments with PB (Fig. 5a), the average values (open squares) of Young's modulus remained constant during pre-exposure times up to 3 h and were reduced significantly from ~ 35 MPa to < 8 MPa after chlorine addition (0.1 mM). In the sequential application of chlorine followed by

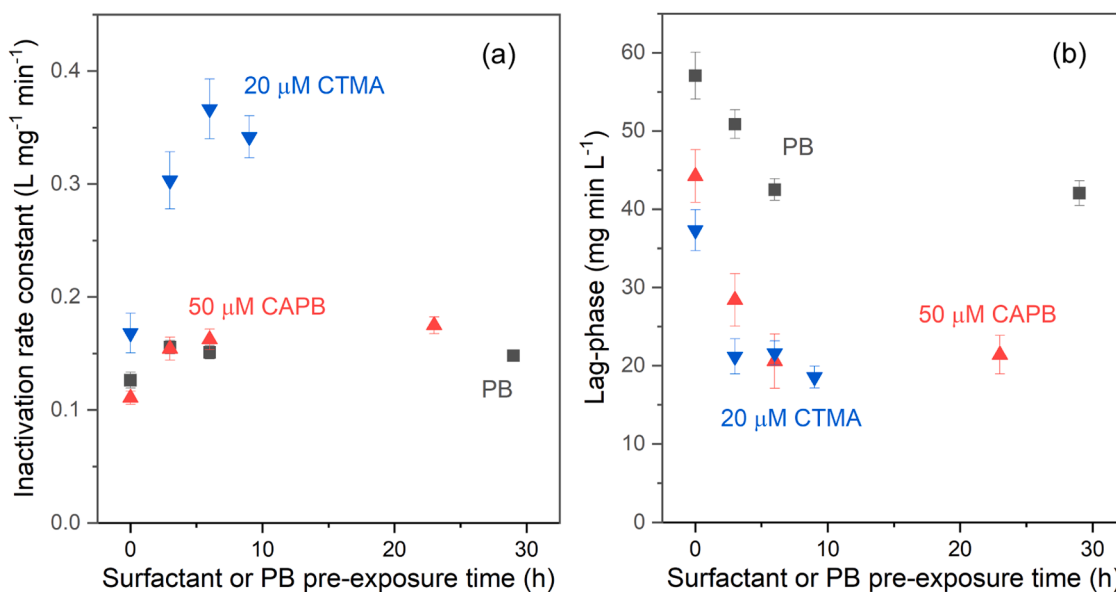


Fig. 3. Inactivation of *B. subtilis* spores during chlorination in absence and presence of surfactants. Effect of the pre-exposure time with CTMA (20 μM , blue triangles) or CAPB (50 μM , red triangles) on (a) second-order inactivation rate constants and (b) lag-phases. Blank experiments with only PB are also shown (black squares). [*B. subtilis* spores]₀ $\approx 5.6 \times 10^5$ CFU/mL (see Table S3 for details), [chlorine]₀ = 7.1 mg/L, 20 mM PB, pH 7.0. Error bars were generated from inactivation kinetics fitting using the package “nlsMicrobio” in R by grouping duplicate experiments.

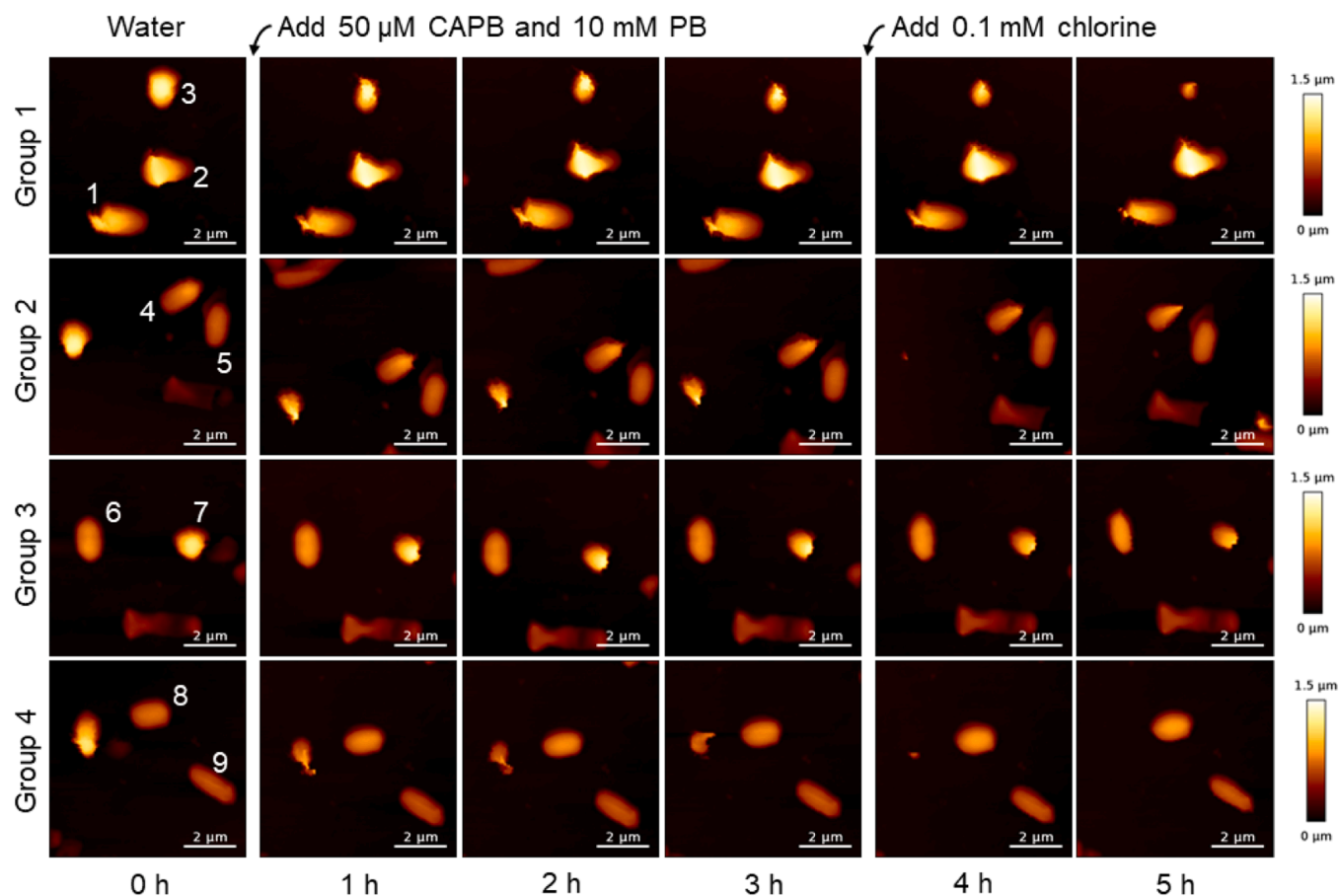


Fig. 4. Atomic Force Microscopy (AFM) height images tracing the morphological changes of individual *B. subtilis* spores for blanks (water, 0 h), pre-treatment with CAPB (50 μM , 1–3 h) in 10 mM PB (pH 7) for 3 h, and post-chlorination (0.1 mM, 4–5 h) for 2 h. The spores labeled with numbers were traced to calculate the evolution of dimensions (length, width, and height), surface roughness, and compressive stiffness.

surfactants (Figs. 5b, c), the mean values (open squares) of Young's modulus decreased gradually from ~ 30 MPa to ~ 18 MPa or ~ 7 MPa after pre-exposing to CAPB or CTMA, respectively. Post-chlorination further reduced the averaged Young's modulus value to ~ 12 MPa for CAPB, no further reduction was observed for CTMA. In a separate test where *B. subtilis* spores were exposed to 50 μM CAPB for 7 h or to 20 μM CTMA for 3 h, Young's modulus values were eventually reduced to the same level (~ 5 MPa) for both CAPB and CTMA (Figure S17).

Considering the structure of *B. subtilis* spores (Figure S1), the decrease in Young's modulus, or compressive stiffness, suggests a less rigid spore coat. Since the coat serves as the first barrier against chemical disinfection, changes in the coat layer could be linked to the reductions in lag-phases observed in inactivation curves. Indeed, the changes in lag-phases (Fig. 3b) and Young's modulus (Figures 5 and S17) for surfactant exposures follow the same trend for the two surfactants. For both parameters, the lag-phases and Young's modulus, CTMA induced more rapid changes than CAPB, but ultimately, CTMA and CAPB were equally effective. These observations strongly suggest that surfactants could alter the coat of the spores during pre-exposure, thereby, reducing lag-phases in post-chlorination.

3.3. Integrity of the inner membrane of *B. subtilis* spores for chlorination or treatment with CTMA

The underlying layers of the coat of spores are largely permeable except the inner membrane which plays an important role in protecting essential genetic material stored in the core (Figure S1) (Setlow 2014). The integrity of the inner membrane can be assessed by detecting the release of DPA which is present in the core and makes up 5–10 % of the

dry weight of bacterial spores (Setlow 1995). To better understand disinfection mechanisms, the required chlorine exposures were compared for the inactivation of spores for loss of viability and for damaging the inner membrane (Fig. 6a). As expected, higher chlorine exposures were necessary to damage the inner membrane and release DPA compared with their inactivation with loss of viability. For chlorination, 90 % of the spores lost viability for a chlorine exposure of 80 $\text{mg}\cdot\text{L}^{-1}\cdot\text{min}$ (black squares). In contrast, only 30 % of the spores lost the integrity of the inner membrane for a chlorine exposure of $\sim 13,000$ $\text{mg}\cdot\text{L}^{-1}\cdot\text{min}$ (Fig. 6a, blue triangles). A post-heating applied to chlorine-treated spores at a sub-lethal temperature (70 $^{\circ}\text{C}$) after quenching the residual chlorine could promote the release of DPA (Figure S8). However, despite post-heating at a chlorine exposure of 80 $\text{mg}\cdot\text{L}^{-1}\cdot\text{min}$, only ~ 14 % of the spores lost the integrity of the inner membrane compared to 90 % loss of viability (Fig. 6a). Therefore, chlorine can inactivate *B. subtilis* spores with limited effects on the inner membrane. This has also been observed for inactivation of bacterial cells with several disinfectants (e.g. ozone, chlorine, chlorine dioxide) for which inactivation occurred before membrane damage (Ramseier et al. 2011). Furthermore, after chlorination the inner membrane became more vulnerable when the temperature was increased. This shows that chlorine modifies the inner membrane, however, does not fully destroy it.

CTMA is also a sporicide and the exposures needed to inactivate the spores and to damage the inner membrane were also assessed (Fig. 6b). With a CTMA exposure of ~ 8500 $\text{mg}\cdot\text{L}^{-1}\cdot\text{min}$, the inactivation efficiency was 99 %, while 22 % of the inner membranes were damaged for these conditions. In general, CTMA could damage the inner membrane of *B. subtilis* spores suggesting different mechanisms than for CAPB or

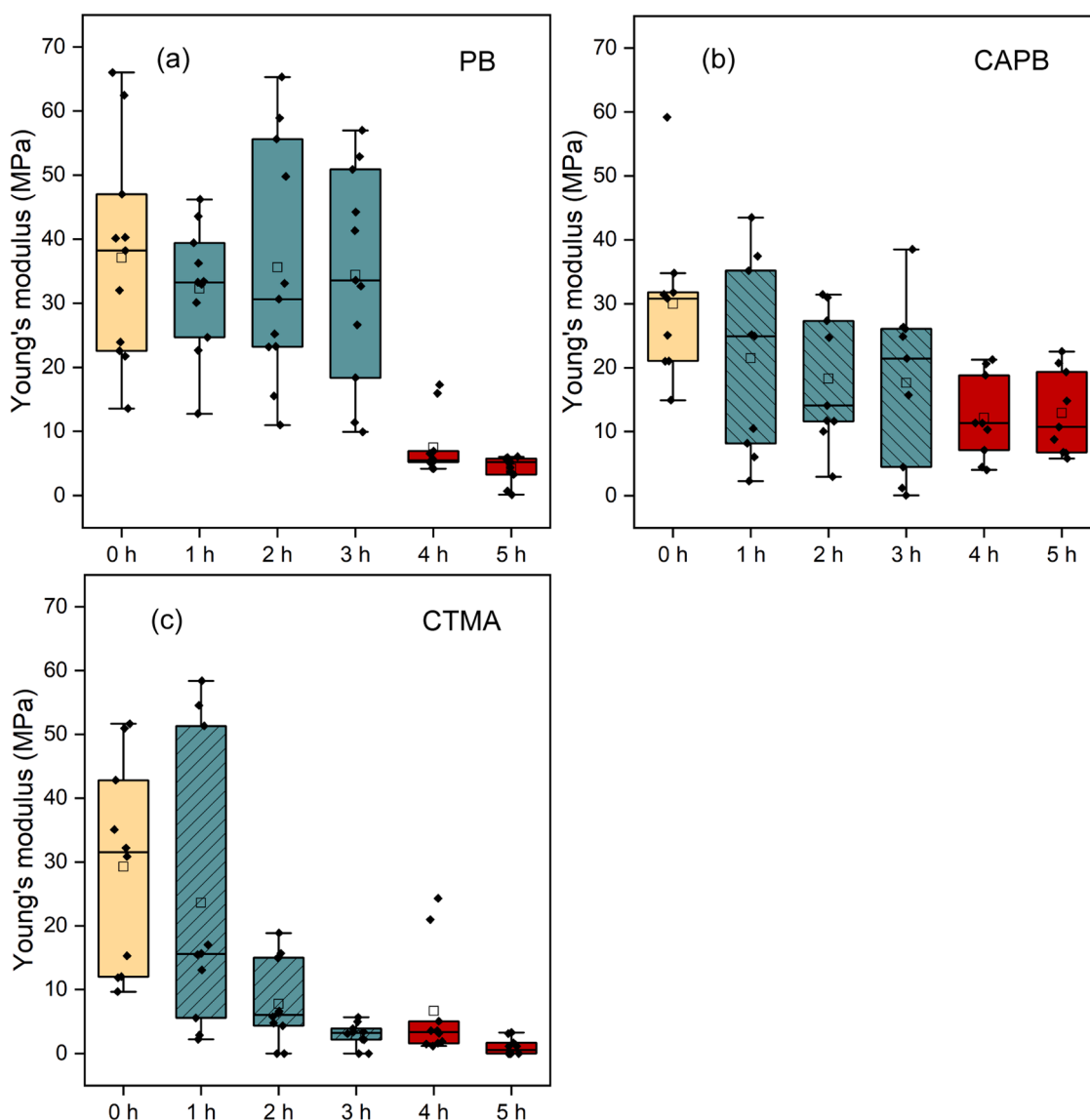


Fig. 5. Changes of Young's modulus as a function of time when tracing the same groups of *B. subtilis* spores for various treatments at pH 7.0: blank in water (0 h, yellow); pre-treatment (1–3 h green) with (a) 10 mM PB, (b) 50 μ M CAPB in 10 mM PB, or (c) 50 μ M CTMA in 10 mM PB for 3 h; and post-chlorination (4–5 h, red) with 0.1 mM chlorine for 2 h. Open squares represent mean values.

chlorine. In addition, different from the inactivation with chlorine (Figure S18), there was no lag-phase during the inactivation of *B. subtilis* spores with CTMA (Figure S19). In contrast, when plotting log-inactivation as a function of the CTMA exposure, inactivation kinetics were faster at the beginning and decreased gradually (Figure S19). The inactivation kinetics of *B. subtilis* spores by CTMA were further investigated by varying the CTMA concentrations (0–100 μ M). The kinetics in both viability (Figure S20) and membrane integrity tests (Figure S21) increased with increasing CTMA concentrations reaching a plateau at about 10 μ M CTMA. Higher concentrations of CTMA were not beneficial in increasing the inactivation kinetics suggesting that the interaction between CTMA and the spores was dominated by surface interactions with a saturation effect beyond which no further enhancement was possible.

Unlike CTMA, CAPB alone was not capable of inactivating *B. subtilis* spores (Figure S10) or damaging the inner membrane (Figure S22) under the tested conditions. In sequential treatment with surfactants followed by chlorination, CTMA, in contrast to CAPB, can partially damage the inner membrane during pre-exposure. This allows chlorine to access the essential genetic materials and proteins stored inside the

inner membrane. The different capabilities in penetrating the spores' inner structures could potentially explain the differences between CTMA and CAPB in enhancing the inactivation rate constants during post-chlorination (Fig. 3a). Overall, CTMA-exposure damaged more layers than CAPB-exposure for chlorine to access.

The combined effects of chlorine and CTMA were also investigated with inner membrane integrity tests. Different from viability tests, a synergistic effect was observed when applying CTMA and chlorine simultaneously instead of sequentially. As shown in Fig. 7, applying 0.5 mM chlorine and 20 μ M CTMA simultaneously (black squares) yielded more efficient lysis of the inner membrane compared to the summation (purple diamonds) of the treatments by 0.5 mM chlorine (red circles) and 20 μ M CTMA (blue triangles) alone. Two other CTMA concentrations (10 and 50 μ M) were tested in the same manner, and the same enhanced lysis of the inner membrane was observed under simultaneous applications (Figure S23). In these experiments, a high concentration (0.5 mM) of chlorine was applied to achieve an apparent membrane lysis under chlorination. In contrast to CTMA, no synergistic effect was observed for a concurrent presence of chlorine and CAPB, and even a reduction of the DPA release rate was observed without post-heating of

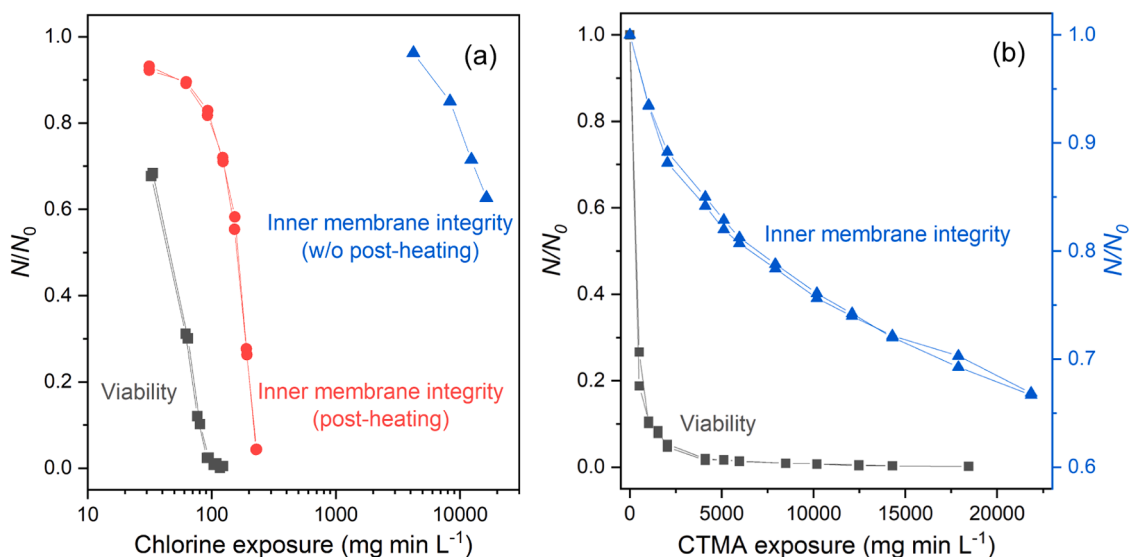


Fig. 6. Relative viability and inner membrane integrity of *B. subtilis* spores as a function of (a) chlorine and (b) CTMA exposure. In inner membrane integrity tests, the number of intact cells was calculated based on the detected concentration of DPA (see Figure S7 for more details). Post-heating was conducted at 70 °C for 30 min (Fig. 6a). Duplicate experiments were plotted separately. In (b), the right Y-axis (blue, linear scale) refers to the inner membrane integrity. [*B. subtilis* spores]₀ ≈ 5.5 × 10⁵ CFU/mL, [chlorine]₀ = 7.1 mg/L (viability and inner membrane integrity with post-heating) or 35.5 mg/L (membrane integrity w/o post-heating), [CTMA]₀ = 2.8 mg/L (10 μM). 20 mM PB for the viability test in (a), 1 mM PB for the membrane integrity tests in (a) and all the tests in (b), pH 7.0.

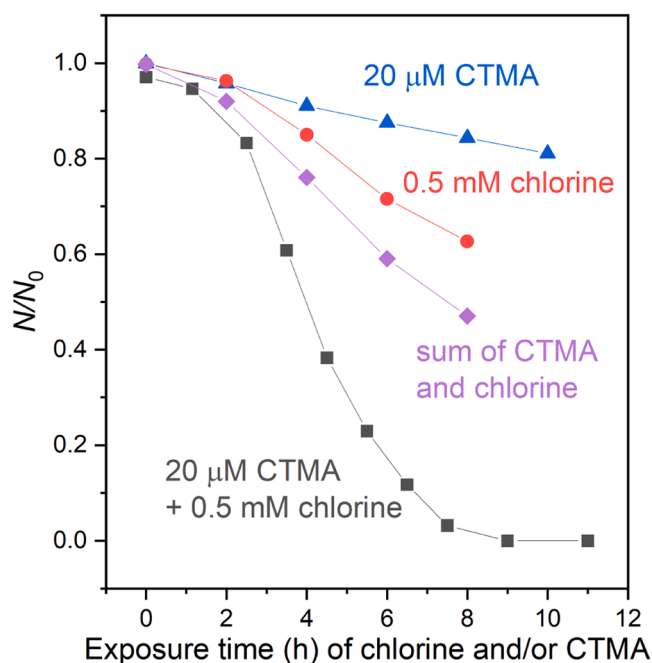


Fig. 7. Relative inner membrane integrity of *B. subtilis* spores as a function of time during exposure to chlorine, CTMA, or a combination of chlorine and CTMA. The number of intact cells was calculated based on the detected concentration of DPA (see Figure S7 for more details). Post-heating was not applied. [*B. subtilis* spores]₀ ≈ 5.5 × 10⁵ CFU/mL, 1 mM PB, pH 7.0.

samples (Figure S24) which needs to be further explored. When applying surfactants and chlorine sequentially, instead of a synergistic effect, a slight reduction in the opening of the inner membrane was observed when the spores were pre-exposed to either CAPB or CTMA in comparison with the PB control (Figure S25). A possible explanation could be that during pre-exposure with surfactants, particularly CTMA, chlorine-reactive constituents were released from the inner core, thereby making post-chlorination less effective. However, this

hypothesis needs to be further investigated.

3.4. Practical implications

Wastewater effluent treated with biological treatment still contains hundreds of μg/L of surfactants from soap (Matthijs et al. 1999). In systems with recycled handwashing water (Hands4health 2022), surfactant concentration can be much higher. The presence of these surfactants can enhance the inactivation efficiency of pathogenic bacteria and bacterial spores during chemical disinfection of municipal wastewater and reused handwashing water. Since the synergistic effects between surfactants and chlorine are suggested to occur due to the increased permeability of the cell membranes to chlorine, this enhancement may also apply to other oxidants that inactivate bacteria and bacterial spores after penetrating the cell membranes, such as chlorine dioxide, chloramine, and peracetic acid (Ramseier et al. 2011, Zhang et al. 2020). In the case of ozone, despite ozone being more reactive than other oxidants, synergistic enhancement of *E. coli* inactivation was also observed when CTMA and ozone were applied simultaneously or sequentially with *E. coli* cultured in CTMA-containing broth before ozonation (Voumard et al. 2022).

Bacterial spores can withstand common disinfection procedures, making them a significant threat when surfaces or areas are contaminated (Barbut and Petit 2001, Whitney et al. 2003). For instance, commercial detergent wipes have shown varied efficacy in removing bacterial spores from clinical surfaces; in many cases, they only transferred spores from one surface to another (Boyce 2021, Siani et al. 2011). Based on the current study, combining different disinfectants, such as CTMA and chlorine, and strategically applying various surfactants and disinfectants in sequence, may offer feasible solutions to control the risks posed by bacterial spores in e.g., the food industry and clinical settings.

4. Conclusions

The combined effects of the surfactants, CAPB or CTMA and chlorine have been investigated for the inactivation of *B. subtilis* spores. The main outcomes of this study are:

- During inactivation of *B. subtilis* spores, synergistic effects for surfactants and chlorine have been observed with shorter lag-phases and/or increasing the second-order inactivation rate constants.
- Compared to chlorine disinfection, a simultaneous application of surfactants and chlorine only resulted in a moderate reduction in the lag-phases for inactivation of spores, and a small increase in the second-order inactivation rate constants was observed.
- Synergistic effects were observed when the spores were pre-exposed to either CAPB or CTMA, with about 50 % decrease in the lag-phases for both CAPB and CTMA and a > 2-fold increase in the second-order inactivation rate constant for CTMA, compared to the PB control group.
- Changes in the mechanical properties of the spores from blank experiments to pre-exposure to surfactants followed by post-chlorination were measured by atomic force microscopy. A significant decrease in compressive stiffness (calculated by the parameter Young's modulus) after pre-exposure to CAPB or CTMA indicates that the surfactants can alter the coat of the spores which is a primary barrier for chemical disinfectants. The changes in the coat could be linked to the reductions of inactivation lag-phases.
- CTMA inactivates *B. subtilis* spores through mechanisms different from chlorine. Chlorine primarily inactivates *B. subtilis* spores before damaging the inner membrane, whereas CTMA damages the inner membrane partially for exposures necessary for inactivation. A synergistic effect in damaging the integrity of the inner membrane was observed when applying CTMA and chlorine simultaneously instead of sequentially. For instance, the simultaneous application of CTMA and chlorine damaged > 90 % of the inner membranes of the spores in 8 h, while the summation of CTMA alone and chlorine alone damaged about 50 % of the inner membranes only.

CRediT authorship contribution statement

Tianqi Zhang: Writing – original draft, Visualization, Validation, Software, Methodology, Investigation, Formal analysis, Data curation, Conceptualization. **María Inés Villalba:** Visualization, Validation, Software, Methodology, Investigation, Formal analysis. **Rongjun Gao:** Software, Methodology, Investigation. **Sandor Kasas:** Software, Resources, Methodology. **Urs von Gunten:** Writing – review & editing, Validation, Supervision, Resources, Methodology, Investigation, Funding acquisition, Formal analysis, Conceptualization.

Declaration of competing interest

The authors declare that they have no known competing financial interests or personal relationships that could have appeared to influence the work reported in this paper.

Acknowledgments

This study was supported by the Swiss Agency for Development and Cooperation (project number 7F-10345.03.01). M.I.V. and S.K. were supported by FWO-SNSF (grant number 310030L_197946) and R. G. was supported by Heyning-Roelli Foundation. We also thank Caroline Gachet-Acquillon for her valuable assistance in the laboratory and Florian Breider for discussions on DPA measurements and AFM analysis.

Supplementary materials

Supplementary material associated with this article can be found, in the online version, at [doi:10.1016/j.watres.2024.122944](https://doi.org/10.1016/j.watres.2024.122944).

Data availability

Data will be made available on request.

References

- Andersson, A., Ronner, U., Granum, P.E., 1995. What problems does the food industry have with the spore-forming pathogens *Bacillus cereus* and *Clostridium perfringens*? *Int. J. Food Microbiol.* 28, 145–155.
- Baird, R., Bridgewater, L., 2017. *Standard Methods for the Examination of Water and Wastewater*. American Public Health Association, Washington, D.C.
- Barbut, F., Petit, J.C., 2001. Epidemiology of *Clostridium difficile*-associated infections. *Clin. Microbiol. Infect.* 7 (8), 405–410.
- Baty, F., Delignette-Muller, M.-L. and Siberchicot, A. (2022) nlsMicrobio: data sets and nonlinear regression models dedicated to predictive microbiology. R package version 0.0-3.
- Birnie, C.R., Malamud, D., Schnaare, R.L., 2000. Antimicrobial evaluation of *N*-alkyl betaines and *N*-alkyl-*N,N*-dimethylamine oxides with variations in chain length. *Antimicrob. Agents Chemother.* 44 (9), 2514–2517.
- Blatchley III, E.R., Meeusen, A., Aronson, A., Brewster, L., 2005. Inactivation of *Bacillus* spores by ultraviolet or gamma radiation. *J. Environ. Eng.* 131 (9), 1245–1252.
- Boyce, J.M., 2021. A review of wipes used to disinfect hard surfaces in health care facilities. *Am. J. Infect. Control* 49 (1), 104–114.
- Bucheli, M., Egli, T., 2010. IUV-Workshop. Standards und Vorschriften bei der UV-Desinfektion von Trinkwasser. *GWA Gas, Wasser, Abwasser* 90 (4), 335–339.
- Cano, R.J., Borucki, M.K., 1995. Revival and identification of bacterial spores in 25- to 40-million-year-old dominican amber. *Science* 268 (5213), 1060–1064.
- Chada, V.G., Sanstad, E.A., Wang, R., Driks, A., 2003. Morphogenesis of *Bacillus* spore surfaces. *J. Bacteriol.* 185 (21), 6255–6261.
- Chauret, C.P., Radziminski, C.Z., Lepuil, M., Creason, R., Andrews, R.C., 2001. Chlorine dioxide inactivation of *Cryptosporidium parvum* oocysts and bacterial spore indicators. *Appl. Environ. Microbiol.* 67 (7), 2993–3001.
- Cho, M., Chung, H., Yoon, J., 2003. Quantitative evaluation of the synergistic sequential inactivation of *Bacillus subtilis* spores with ozone followed by chlorine. *Environ. Sci. Technol.* 37 (10), 2134–2138.
- Cho, M., Kim, J.H., Yoon, J., 2006. Investigating synergism during sequential inactivation of *Bacillus subtilis* spores with several disinfectants. *Water. Res.* 40 (15), 2911–2920.
- Clara, M., Scharf, S., Scheffknecht, C., Gans, O., 2007. Occurrence of selected surfactants in untreated and treated sewage. *Water. Res.* 41 (19), 4339–4348.
- Cortezzo, D.E., Setlow, P., 2005. Analysis of factors that influence the sensitivity of spores of *Bacillus subtilis* to DNA damaging chemicals. *J. Appl. Microbiol.* 98 (3), 606–617.
- Dong, W., Green, J., Korza, G., Setlow, P., 2019. Killing of spores of *Bacillus* species by cetyltrimethylammonium bromide. *J. Appl. Microbiol.* 126 (5), 1391–1401.
- Driedger, A., Staub, E., Pinkernell, U., Marinas, B., Koster, W., von Gunten, U., 2001. Inactivation of *Bacillus subtilis* spores and formation of bromate during ozonation. *Water Res.* 35 (12), 2950–2960.
- Driks, A., 1999. *Bacillus subtilis* spores coat. *Microbiol. Mol. Biol.* 63 (1), 1–20.
- El-Dossoki, F.I., Abdalla, N.S.Y., Gomaa, E.A., Hamza, O.K., 2020. An insight into thermodynamic and association behaviours of cocamidopropyl betaine (CAPB) surfactant in water and water–alcohol mixed media. *SN Appl. Sci.* 2 (4).
- Falk, N.A., 2019. Surfactants as antimicrobials: a brief overview of microbial interfacial chemistry and surfactant antimicrobial activity. *J. Surfactants. Deterg.* 22 (5), 1119–1127.
- Geeraerd, A.H., Valdramidis, V.P., Van Impe, J.F., 2005. GlnaFit, a freeware tool to assess non-log-linear microbial survivor curves. *Int. J. Food Microbiol.* 102 (1), 95–105.
- Glover, R.E., Smith, R.R., Jones, M.V., Jackson, S.K., Rowlands, C.C., 1999. An EPR investigation of surfactant action on bacterial membranes. *FEMS Microbiol. Lett.* 177, 57–62.
- Goronja, J., Janosevic-Lezaic, A., Dimitrijevic, B., Malenovic, A., Stanisavljevic, D., Pejic, N., 2016. Determination of critical micelle concentration of cetyltrimethylammonium bromide: Different procedures for analysis of experimental data. *Hem. Ind.* 70 (4), 485–492.
- Hands4health (2022) Hand hygiene, water quality and sanitation in primary health care facilities and schools not connected to functional water supply systems, accessed 11 July 2024, <<https://hands4health.dev/>>.
- Henriques, A.O., Melsen, L.R., Moran, C.P., 1998. Involvement of superoxide dismutase in spore coat assembly in *Bacillus subtilis*. *J. Bacteriol.* 180 (9), 2285–2291.
- Henriques, A.O., Moran Jr, C.P., 2007. Structure, assembly, and function of the spore surface layers. *Annu. Rev. Microbiol.* 61, 555–588.
- Hindle, A.A., Hall, E.A.H., 1999. Dipicolinic acid (DPA) assay revisited and appraised for spore detection. *Analyst* 124, 1599–1604.
- Kelleppan, V.T., King, J.P., Butler, C.S.G., Williams, A.P., Tuck, K.L., Tabor, R.F., 2021. Heads or tails? The synthesis, self-assembly, properties and uses of betaine and betaine-like surfactants. *Adv. Colloid Interface Sci.* 297, 102528.
- Kumar, K., Margerum, D.W., 1987. Kinetics and mechanism of general-acid-assisted oxidation of bromide by hypochlorite and hypochlorous acid. *Inorg. Chem.* 26 (16), 2706–2711.
- Larson, M.A., Marinas, B.J., 2003. Inactivation of *Bacillus subtilis* spores with ozone and monochloramine. *Water. Res.* 37, 833–844.
- Leffler, D.A., Lamont, J.T., 2015. *Clostridium difficile* infection. *N. Engl. J. Med.* 372 (16), 1539–1548.
- Leggett, M.J., McDonnell, G., Denyer, S.P., Setlow, P., Maillard, J.Y., 2012. Bacterial spore structures and their protective role in biocide resistance. *J. Appl. Microbiol.* 113 (3), 485–498.
- Margot, J., Rossi, L., Barry, D.A., Holliger, C., 2015. A review of the fate of micropollutants in wastewater treatment plants. *WIRES Water* 2 (5), 457–487.

- Mathijs, E., Holt, M.S., Kiewiet, A., Rijs, G.B.J., 1999. Environmental monitoring for linear alkylbenzene sulfonate, alcohol ethoxylate, alcohol ethoxy sulfate, alcohol sulfate, and soap. *Environ. Toxicol. Chem.* 18 (11), 2634–2644.
- McKenney, P.T., Driks, A., Eichenberger, P., 2013. The *Bacillus subtilis* endospore: assembly and functions of the multilayered coat. *Nat. Rev. Microbiol.* 11 (1), 33–44.
- Melly, E., Cowan, A.E., Setlow, P., 2002. Studies on the mechanism of killing of *Bacillus subtilis* spores by hydrogen peroxide. *J. Appl. Microbiol.* 93, 316–325.
- Mi, L., White, A.D., Shao, Q., Setlow, P., Li, Y., Jiang, S., 2014. Chemical insights into dodecylamine spore lethal germination. *Chem. Sci.* 5 (8), 3320–3324.
- Moore, N., Ebrahimi, S., Zhu, Y., Wang, C., Hofmann, R., Andrews, S., 2021. A comparison of sodium sulfite, ammonium chloride, and ascorbic acid for quenching chlorine prior to disinfection byproduct analysis. *Water Supply* 21 (5), 2313–2323.
- Morrison, C.M., Hogard, S., Pearce, R., Gerrity, D., von Gunten, U., Wert, E.C., 2022. Ozone disinfection of waterborne pathogens and their surrogates: A critical review. *Water. Res.* 214, 118206.
- Nicholson, W.L., Munakata, N., Horneck, G., Melosh, H.J., Setlow, P., 2000. Resistance of *Bacillus* endospores to extreme terrestrial and extraterrestrial environments. *Microbiol. Mol. Biol.* 64 (3), 548–572.
- Otzen, D., 2011. Protein-surfactant interactions: a tale of many states. *Biochim. Biophys. Acta* 1814 (5), 562–591.
- Piret, J., Désormeaux, A., Bergeron, M.G., 2002. Sodium lauryl sulfate, a microbicide effective against enveloped and nonenveloped viruses. *Curr. Drug Targets.* 3 (1), 17–30.
- Ramseier, M.K., von Gunten, U., Freihofer, P., Hammes, F., 2011. Kinetics of membrane damage to high (HNA) and low (LNA) nucleic acid bacterial clusters in drinking water by ozone, chlorine, chlorine dioxide, monochloramine, ferrate(VI), and permanganate. *Water. Res.* 45 (3), 1490–1500.
- Riesenman, P.J., Nicholson, W.L., 2000. Role of the spore coat layers in *Bacillus subtilis* spore resistance to hydrogen peroxide, artificial UV-C, UV-B, and solar UV radiation. *Appl. Environ. Microbiol.* 66 (2), 620–626.
- Rode, L.J., Foster, J.W., 1961. Germination of bacterial spores with alkyl primary amines. *J. Bacteriol.* 81, 768–779.
- Russell, A.D., 1990. Bacterial spores and chemical sporicidal agents. *Clin. Microbiol. Rev.* 3 (2), 99–119.
- Setlow, P., 1993. Binding of small, acid-soluble spore proteins to DNA plays a significant role in the resistance of *Bacillus subtilis* spores to hydrogen peroxide. *Appl. Environ. Microbiol.* 59 (10), 3418–3423.
- Setlow, P., 1995. Mechanisms for the prevention of damage to DNA in spores of *Bacillus* species. *Annu. Rev. Microbiol.* 49, 29–54.
- Setlow, P., 2003. Spore germination. *Curr. Opin. Microbiol.* 6 (6), 550–556.
- Setlow, P., 2006. Spores of *Bacillus subtilis*: their resistance to and killing by radiation, heat and chemicals. *J. Appl. Microbiol.* 101 (3), 514–525.
- Setlow, P., 2014. Spore resistance properties. *The Bacterial spore: From molecules to systems*. Edited by P. Eichenberger and A. Driks *Microbiol. Spectr.* 2 (5), 201–215.
- Sharma, P., Vaiwala, R., Parthasarathi, S., Patil, N., Verma, A., Waskar, M., Raut, J.S., Basu, J.K., Ayappa, K.G., 2022. Interactions of surfactants with the bacterial cell wall and inner membrane: Revealing the link between aggregation and antimicrobial activity. *Langmuir* 38 (50), 15714–15728.
- Siani, H., Cooper, C., Maillard, J.Y., 2011. Efficacy of "sporicidal" wipes against *Clostridium difficile*. *Am. J. Infect. Control* 39 (3), 212–218.
- Sneath, P.H.A., 1962. Longevity of micro-organisms. *Nature* 195 (4842), 643–646.
- Sunde, E.P., Setlow, P., Hederstedt, L., Halle, B., 2009. The physical state of water in bacterial spores. *PNAS* 106 (46), 19334–19339.
- USEPA (2006) **Ultraviolet Disinfection Guidance Manual**, Washington, DC.
- Vepachedu, V.R., Setlow, P., 2007. Role of SpoVA proteins in release of dipicolinic acid during germination of *Bacillus subtilis* spores triggered by dodecylamine or lysozyme. *J. Bacteriol.* 189 (5), 1565–1572.
- Vinckier, A., Semenza, G., 1998. Measuring elasticity of biological materials by atomic force microscopy. *FEBS Lett.* 430, 12–16.
- Voumard, M., Breider, F., von Gunten, U., 2022. Effect of cetyltrimethylammonium chloride on various *Escherichia coli* strains and their inactivation kinetics by ozone and monochloramine. *Water. Res.* 216, 118278.
- Voumard, M., Venturilli, L., Borgatta, M., Croxatto, A., Kasas, S., Dietler, G., Breider, F., von Gunten, U., 2020. Adaptation of *Pseudomonas aeruginosa* to constant sub-inhibitory concentrations of quaternary ammonium compounds. *Environ. Sci. Water Res. Technol.* 6 (4), 1139–1152.
- Wells-Bennik, M.H., Eijlander, R.T., den Besten, H.M., Berendsen, E.M., Warda, A.K., Krawczyk, A.O., Nierop Groot, M.N., Xiao, Y., Zwietering, M.H., Kuipers, O.P., Abee, T., 2016. Bacterial spores in food: Survival, emergence, and outgrowth. *Annu. Rev. Food Sci. Technol.* 7, 457–482.
- Whitney, E.A.S., Beatty, M.E., Taylor Jr, T.H., Weyant, R., Sobel, J., Arduino, M.J., Ashford, D.A., 2003. Inactivation of *Bacillus anthracis* spores. *Emerg. Infect. Dis.* 9 (6), 623–627.
- Young, S.B., Setlow, P., 2003. Mechanisms of killing of *Bacillus subtilis* spores by hypochlorite and chlorine dioxide. *J. Appl. Microbiol.* 95 (1), 54–67.
- Young, S.B., Setlow, P., 2004. Mechanisms of *Bacillus subtilis* spore resistance to and killing by aqueous ozone. *J. Appl. Microbiol.* 96 (5), 1133–1142.
- Yuen, J.W., Chung, T.W., Loke, A.Y., 2015. Methicillin-resistant *Staphylococcus aureus* (MRSA) contamination in bedside surfaces of a hospital ward and the potential effectiveness of enhanced disinfection with an antimicrobial polymer surfactant. *Int. J. Environ. Res. Public Health* 12 (3), 3026–3041.
- Zhang, T., Wang, T., Mejia-Tickner, B., Kisse, J., Xie, X., Huang, C.H., 2020. Inactivation of bacteria by PAA combined with UV irradiation: mechanism and optimization. *Environ. Sci. Technol.* 54, 9652–9661.
- Zolock, R.A., Li, G., Bleckmann, C., Burggraf, L., Fuller, D.C., 2006. Atomic force microscopy of *Bacillus* spore surface morphology. *Micron* 37 (4), 363–369.